SUBSURFACE TOMOGRAPHY IMAGING AT SUB-TERAHERTZ AND TERAHERTZ FREQUENCY

Vertiy A.A., Cetinkaya H., Tekbas M.
International Laboratory for High Technology, Material Institute
TUBITAK-MRC, Gebze / Kocaeli, Turkey
Alex.Vertii@mam.gov.tr, harun.cetinkaya@mam.gov.tr, mustafa.tekbas@mam.gov.tr
Tel : 0090 262 677 3015, Tel : 0090 262 677 3023, Tel : 0090 262 677 3061

Development of millimeter and sub-millimeter wavelengths technologies is one of the most promising research areas, especially for applications in so called terahertz imaging. In the paper we consider a tomography approach for obtaining 3-D imaging in frequency range from 100 GHz up to 325 GHz. We apply the modernized image reconstruction method, based on developed earlier, for low frequency, surface imaging procedure [1]. We managed to significantly improve the image resolution by newly designed probes for millimeter and sub-millimeter wave range measurements. The images obtained demonstrate that the built measurement system and the image reconstruction method can be used for non-destructive testing applications such as the imaging of manufacturing defect on wafer.

Introduction

In a view of growing importance of surface and subsurface imaging, for example, in medical and non-destructive testing, the tomography technologies have been receiving a proper attention [1, 2]. For higher resolution imaging, the changeover to high frequencies is required. Our paper is devoted to development of the sub-terahertz and terahertz tomography that allows us to get quite clear imagine.

TUBITAK - International Laboratory for High Technology have already realized millimeter wave tomography application [3-5]. In this study, the tomography method that we employ, based on evaluating of the distribution of equivalent currents induced on the target, was originally proposed and verified at frequency 3 GHz in the work [1]. We built the microwave measurement setup and successfully used the method in 10 GHz and 40 GHz rangers for surface and subsurface tomography imaging in non-destructive testing and biological applications. Herein it is shown that similar method can give good results also at sub-terahertz (100 GHz) and terahertz (325 GHz) frequencies for surface and subsurface applications. The essential resolution improvement in W band was achieved with using newly designed dielectric probes. The experimental results obtained at the sub-millimeter wave band demonstrate the wide practical application of the method and the proposed measurement setup.

Problem Formulation

Let us consider a three-dimensional object of volume V that is illuminated by a plane linearly polarized wave of E-polarization ($E_{||}$); the wave incident angle is θ^i. The surrounding isotropic medium is supposed uniform and defined by its permittivity ε and conductivity σ. The media permeability is $\mu = 1$.

Let $\vec{E}$ represent the total electric field, $\vec{E}^i$ is an incident field and $\vec{E}^s$ is a scattered field which is excited by the equivalent electric currents (polarization currents), so $\vec{E} = \vec{E}^i + \vec{E}^s$. The equivalent electric currents are defined as

$$\vec{J}_{ob}(x,y,z) = (k_{ob}^2(x,y,z) - k^2)\vec{E}(x,y,z) \tag{1.1}$$

where k_{ob} and k are the wave numbers for the object medium and vacuum correspondently, the time dependence is chosen in the form $e^{-i\omega t}$.

The scattered field $\vec{E}^s_{||}$, that is parallel to z, inside and outside the object can be calculated by using its integral representation. If one assumes that the depolarization is negligible, and polarization current is normalized by incident field $E^i_z(\theta^i, x, y)$, the scattered field $\psi\left(\theta^i, x, y, z\right)$ can be presented in the form

$$\psi(\theta^i, x, y, z) = k^2 \iiint_V E^i_z(\theta^i, x', y') K(\theta^i, x', y', z') G(x, y, z; x', y', z') dx' dy' dz' \tag{2}$$

where $G(x, y, z; x', y', z')$ is free space Green function, $K(\theta^i, x', y', z')$ is a normalized polarization current and $E^i_z(\theta^i, x, y) = e^{ik(x\sin\theta^i + y\cos\theta^i)}$ is an incident plane wave.

978-1-4244-7899-6/10/$26.00 ©2010 IEEE

Let us define the two-dimensional Fourier transform $\hat{\psi}\left(\theta^i, v_1, y, v_3\right)$ of the scattered field $\psi\left(\theta^i, x, y, z\right)$ on a scanning plane at y=constant and also the three-dimensional Fourier transform $\hat{K}(\theta^i, \alpha, \beta, \chi)$ of $K\left(\theta^i, x, y, z\right)$

$$\hat{\psi}\left(\theta^i, v_1, y, v_3\right) = \int_{-\infty}^{\infty}\int_{-\infty}^{\infty} \psi(\theta^i, x, y, z) e^{-2\pi i\left(v_1 x + v_3 z\right)} dxdz \tag{3}$$

$$\hat{K}(\theta^i, \alpha, \beta, \chi) = \int_{-\infty}^{\infty}\int_{-\infty}^{\infty}\int_{-\infty}^{\infty} K(\theta^i, x, y, z) e^{-2\pi i(\alpha x + \beta y + \chi z)} dxdydz. \tag{4}$$

Applying the two-dimensional Fourier transform for (2) along x and z directions, one can obtain the following equation:

$$\hat{\psi}\left(\theta^i, v_1, y, v_3\right) = k^2 \int_{-\infty}^{\infty}\int_{-\infty}^{\infty}\int_{-\infty}^{\infty} e^{ik\left(x'\sin\theta^i + y'\cos\theta^i\right)} K(\theta^i, x', y', z') \underbrace{\frac{i}{2}\frac{e^{-2\pi i v_1 x'} e^{i\gamma(y'-y)} e^{-2\pi i v_3 z'}}{\gamma}}_{g(v_1, y, v_3; x', y', z')} dx'dy'dz' \tag{5}$$

where $g(v_1, y, v_3; x', y', z')$ is the two-dimensional Fourier transform of Green function, and $\gamma = 2\pi v_2 = \sqrt{k^2 - 4\pi^2\left(v_1^2 + v_3^2\right)}$ is the wave number.

After some manipulations, the equation (5) becomes

$$\hat{K}(\theta^i, \alpha, \beta, \chi) = \hat{\psi}\left(\theta^i, v_1, y, v_3\right)\frac{2\gamma}{k^2 i e^{-i\gamma y}}, \tag{6}$$

where α, β, and χ have the following presentations

$$\alpha = v_1 - \frac{k}{2\pi}\sin\theta^i,\ \beta = -\frac{1}{2\pi}\left(\gamma + k\cos\theta^i\right),\ \chi = v_3 \tag{7}$$

Experimental Setup And Applications

Our measurement system includes the specially designed PNA Control Software, installed in control computer for scanner system data acquisition, to be able to control all measurement setup, network analyzer (Agilent PNA N5260A), Probe Station (Cascade Probstation, summit 12000 B-S), and Scanner-Positioner Control Computer (see Figure 1). Thus, control computer for scanner system data acquisition performs a role of master computer. In our design the Scanner-Positioner Control Computer only controls the Scanner-Positioner System. Also, data acquisition over $x - y$ scan area on the object is performed by PNA Control Software. The Probe Station Positioner goes to the coordinate point, assigned by PNA Control Software, to make a measurement. In a such way the measured data is collected. Moreover, the measurement is processed by using the network analyzer for different frequencies. During these experiments, all of measurements are made at 32 different frequencies with a constant frequency step. We use the frequency range [98 GHz, 102 GHz] for millimeter wave measurements. Sub-millimeter wave measurements are conducted in the interval from 300 GHz to 320 GHz.

The crucial component of our experimental setup is dielectric probes. Figure 1 - (b) shows the W-band dielectric probe, made from Teflon. We used it for millimeter wave measurements. In Figure 1- (c) a dielectric probe, made from Duroid and inserted into the horn antenna, was used at sub-millimeter wave measurements.

For subsurface measurements at millimeter wave range one object was used. The object was cardboard capital letter C shown in Figure 2 (a) and (b), the height, width and thickness of which were 40 mm, 40 mm, and 0.8 mm, respectively.

Also, at millimeter wave range, the surface measurement of copper capital letter A, placed on FR4 PCB, (Figure 2 (c) and (d)), was performed. Its dimensions are the height of 5.78 mm, the width of 9.81 mm, and the FR4 PCB thickness of 1 mm.

At a sub-millimeter wave region, the subsurface tomography measurements was made for a similar object, copper capital letter A on FR4 PCB (see Figure 2 (c) and (d)).

It should be indicated that thicknesses of Teflon, used as layers for millimeter and sub-millimeter wave measurements, were 5 mm and 3 mm, respectively.

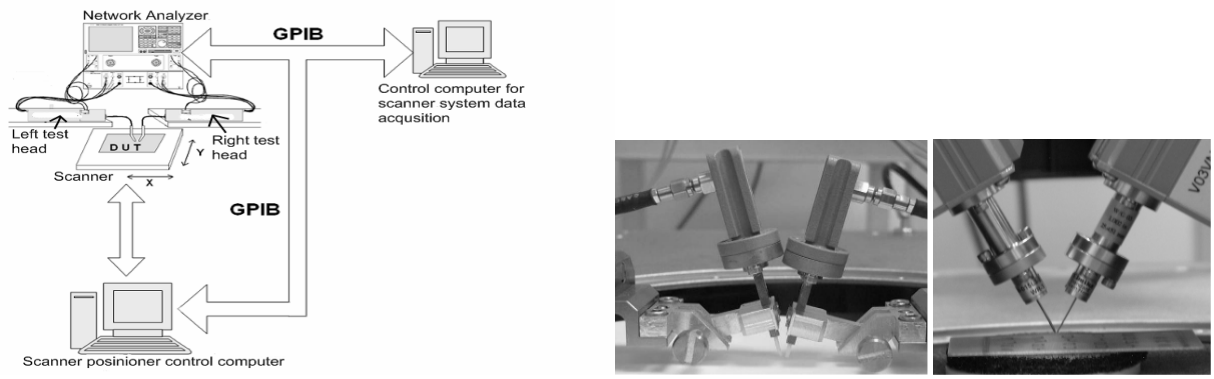

(a) (b) (c)

Figure 1. (a) - the measurement system and designed probes for measurements at (b)-100 GHz and at (c)- 300 GHz.

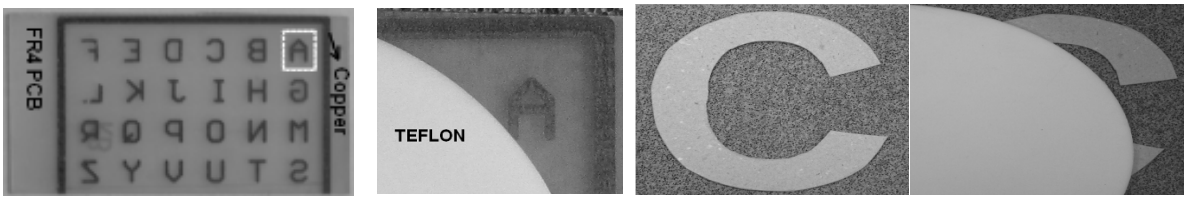

(a) (b) (c) (d)

Figure 2. (a) - cardboard capital letter C and (b) - cardboard capital letter C under Teflon, (c) - copper capital letter A , placed on FR4 PCB and (d) - copper capital letter A, placed on FR4 PCB, under Teflon.

Experimental Results

Firstly, note that measurement plane consisted of 100×100 grids in the measurement. One grid size was 0.5×0.5 mm^2 in millimeter wave measurement for cardboard capital letter C. For capital letter A on FR4 PCB, one grid size was 25×25 mm^2 at both of measurement frequency ranges. The 3-D image visualization was done by using IRIS Explorer™ software [6].

The measured data and subsurface tomography reconstruction for cardboard letter C are shown in Figure 3. The measurement data of copper capital letter A on FR4 PCB, measured as a surface measurement object at millimeter wave region, is shown in Figure 2 - (c).

The measured data and tomography reconstructions for subsurface imagine of copper capital letter A on FR4 PCB at sub-millimeter wave region are shown in Figure 5.

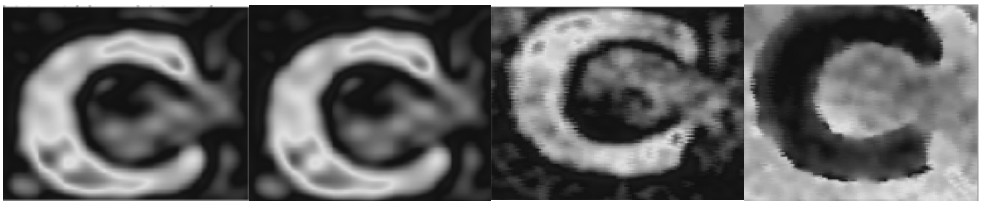

(a) (b) (c) (d)

Figure 3. (a) - amplitude and (b) - phase distributions and the tomography reconstruction for depths of (c) - 0.001 m and (d) - 0.002 m, for cardboard object at 98GHz - 102 GHz.

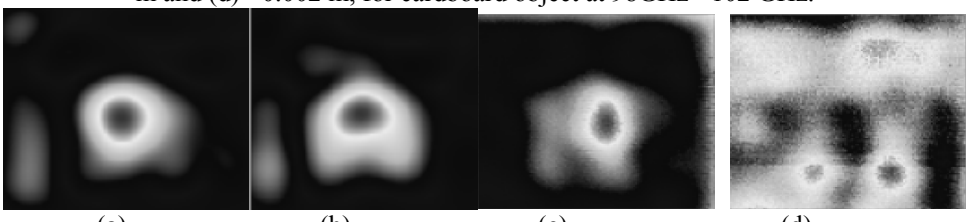

(a) (b) (c) (d)

Figure 4. (a) - amplitude, (b) - phase distribution and the tomography reconstruction for depths of (c) - 0.00025 m and (d) - 0.001 m, for copper capital letter A placed on FR4 PCB at 98GHz - 102 GHz.

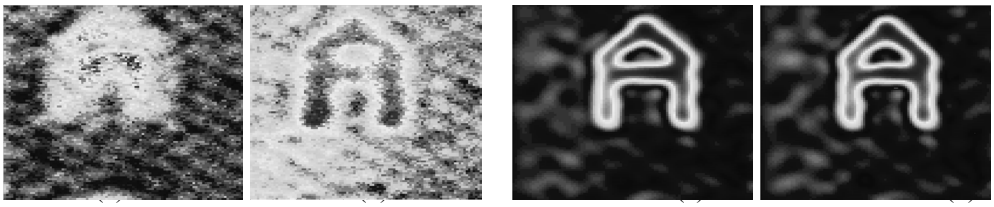

Figure 5. (a) - amplitude, (b) - phase distributions and the tomography reconstruction for depths of (c) - 0.003 m and (d) - 0.004 m for copper capital letter A placed on FR4 PCB at 300 GHz - 320 GHz.

Conclusion

The dielectric objects are more difficult for measurement because of the scattered field produced by a dielectric object is much weaker than that produced by metallic object. We present the image reconstruction of a dielectric object, cardboard capital letter C at millimeter wave region. It demonstrates that accurate scattering data is able to be collected from dielectric target and high quality images can be generated.

Also, at millimeter wave region it can be seen from the measurement results of copper capital letter A on FR4 PCB (see Figure 4 - (a) and (b)) that its amplitude and phase distributions are not satisfying. Thus, the resolutions of the reconstruction results of the object are not good (see Figure 4 - (c) and (d)). Even though, at sub-millimeter wave region the measured data and reconstruction results for the similar object are much better in contrast with those at millimeter wave region. A difference between reconstruction results at millimeter and sub-millimeter wave regions is due to the wave length. Because the wave length at sub-millimeter wave region is three times smaller than the wave length at millimeter wave region.

Beside, the experimental setup was designed and built for sub-terahertz and terahertz frequencies measurements. This imaging system and reconstruction algorithm have demonstrated good results to be used for different types of technological and scientific applications. Thus, our further studies will be focused non-destructive imaging and wafer imaging which is important for non-destructive control system to detect manufacturing defect on wafer.

References

1. Pichot C., L. Jofre, G. Perronnet, J.C. Bolomey, Active Microwave Imaging of Inhomogeneous Bodies, IEEE Transaction On Antenna And Propagation, vol. Ap-33, No. 4, pp. 416-423, April 1985.
2. Candy J.V., C. Pichot, Active Microwave Imaging : A Model-Based Approach, IEEE Transaction On Antenna And Propagation, vol. 39, No. 3, pp. 285-290, March 1991.
3. A.A. Vertiy, S.P. Gavrilov, S. Aksoy, I.V. Voynovskyy, A.M. Kudelya,& V.N. Stepanyuk, Reconstruction of microwave images of the subsurface objects by diffraction tomography and stepped-frequency radar methods, Zarubejnaya Radioelektronika. Uspehi Sovremennoy Radioelektroniki, 7: 17-52, 2001.
4. A.A. Vertiy, S.P. Gavrilov, I.V. Voynovskyy, V.N. Stepanyuk, & S. Ozbek, The millimeter wave tomography application for the subsurface imaging, International Journal of Infrared and Millimeter Waves. 23(10): 1413-1444, 2002.
5. A.A. Vertiy, S.P. Gavrilov, Application of tomography method in millimeter wavelengths band II. Experimental. International Journal of Infrared and Millimeter Waves. 18(9):1761- 1781, 1997.
6. http://www.nag.co.uk/Welcome_IEC.asp